IN-PLANE AND BIAXIAL PERFORMANCE OF SEISMIC PRECAST HOLLOW CORE WALL WITH DIFFERENT TYPES OF ENERGY DISSIPATORS

NOR HAYATI ABDUL HAMID[*]

Abstract. Two geometrically identical seismic precast hollow core walls with foundation beams were constructed and tested under in-plane, out of plane and biaxial loading on shaking table. Both of the walls were steel-armoured at bottom with steel channel and allowed to rock on steel plate located on top of foundation beams. Wall 1 was designed with fixed location of unbonded tendons and a pair of bonded fuse-bar was inserted into the foundation beam. Wall 2 was designed with some flexibility of locations, cross-sectional areas, initial prestressing of unbonded tendons and fuse-bars. Four different combinations of unbonded tendons, unbonded fuse-bars and mechanical energy dissipators were tested using Wall 2. The experimental results showed that Wall 2 performed better than Wall 1 under different load paths without any damage and residual drift. The stiffness of the wall is significantly influenced by the level of initial prestressing, location and cross-sectional area of energy dissipators and unbonded tendons. Fuse-bar with 50% initial prestressing force is recommended because it works efficiently under reverse cyclic loading whereby buckling and plastic hinge zone can be prevented.

Keyword: In-plane loading, biaxial loading, damage, cyclic loading, plastic hinge zone

Abstrak. Sebanyak dua buah *precast hollow core* dinding yang mempunyai geometri yang sama telah dibina berserta dengan tapak asas untuk diuji dengan daya selari mendatar, daya bertentangan dan dwi-daya yang berbentuk dua, empat dan lapan kelopak bunga di atas *shaking table*. Kedua-dua dinding itu telah dimasukkan ke dalam keluli berbentuk 'C' dan diletakkan ke atas kepingan keluli. Model 1 telah direka dengan meletakkan *unbonded tendons* dan *fuse-bar* ke dalam tapak asas manakala Model 2 telah direka bentuk dengan menggunakan beberapa jenis *energy dissipator* berserta dengan *unbonded tendon*. Empat gabungan antara *energy dissipator* dan *unbonded tendon* telah direka, dibina dan diuji di dalam makmal. Keputusan makmal menunjukkan bahawa kedua-dua model tidak mengalami sebarangan kerosakan dan keretakan. Daripada uji kaji ini, 50% daripada *initial prestressing unbonded tendons* telah dipilih kerana menunjukkan keputusan yang paling terbaik di mana tiada keretakan pada model dan kebengkokan pada *fuse-bar*.

Kata kunci: Daya mendatar, dwi-daya, kerosakan, daya yang berputar, zon sangga plastik

1.0 INTRODUCTION

Principally, the main criterion in designing seismic resistant buildings is to maintain life safety of the people even though some damage is permitted. Aftermath of past earthquakes had shown that good seismic

---

[*] Faculty of Civil Engineering, Universiti Teknologi MARA, Shah Alam 4130, Selangor, Malaysia

performance of buildings can be achieved using precast prestressed concrete components and shear walls as the primary in-plane lateral load resisting system [1-3]. Previous study conducted by Fintel [1] in the past 30 years showed that the reinforced concrete buildings containing shear walls performed better than other buildings types. The first major destruction of tilt-up buildings occurred during 1964 Alaska Earthquake where several tilt-up buildings had collapsed including Elmendorf Air Force Base, Anchorage, Alaska [4]. Another major disaster was the 1988 Armenia Earthquake which caused extensive damage to precast concrete frame buildings. Out of 133 buildings of this type, 72 had collapsed and another 55 were heavily damaged and had to be demolished. In Turkey, precast concrete buildings have become popular for manufacturing, agricultural warehouses and commercial buildings with wider spans up to 20 m. Many of these buildings had collapsed during the August 17, 1999 Turkey Earthquake due to instability problems where excessive diaphragm deflections in the portion of building lacking interior partitions led to out-of-plane failure.

The main objective of this research is to investigate the seismic performance of a single precast hollow core wall under quasi-static bi-directional lateral loading including the effects of gravity load. A sufficient vertical loading was applied by putting concrete block on top of precast hollow core wall. Therefore, this research extends the work of Holden [5] by substituting conventional solid reinforced concrete precast panels with precast hollow core panels that possess only minimal longitudinal prestressed strands and no other reinforcement. The challenge of this research is to ensure that this class of precast wall without transverse reinforcement can behave well under seismic loading conditions with minor damage to non-structural and without any damage to structural components. As demonstrated by Holden [5], a good seismic performance of precast wall systems can be achieved by avoiding the formation of plastic hinge at the bottom of wall through disconnecting the wall-foundation interface and clamping them together using unbonded tendons. If the steel armouring is used at the wall base, then the damage to the precast panels can be avoided. One of the fundamental differences between this research and that of Holden [5] is that the tapered energy dissipators cannot be replaced after it yield or fractured but with unbonded fuse-bars, it easily replaced or restressed after an extreme ground shaking.

2.0   DESIGN AND CONSTRUCTION OF THE WALL SPECIMENS

Figure 1 shows the conceptual design of a prototype warehouse where it is envisaged precast hollow core wall units used as the principal structural and cladding elements. The "seismic walls" is designed to carry gravity, seismic and winds loads from the roof. It is designed according to Damage Avoidance Design philosophy proposed by Mander and Cheng [6].
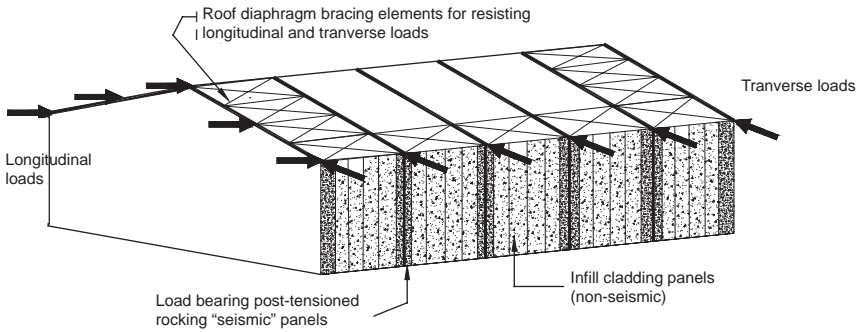
Figure 1   The conceptual design of "seismic wall" in warehouse building

Figure 2 shows the overall idealised force vs deformation seismic behaviour of a rocking precast hollow core units using unbonded tendons and energy dissipators. The rocking seismic precast hollow core wall can be modelled as a SDOF system where the combined behaviour of unbonded tendons and gravity load behave as Bi-Linear Elastic elements as shown in Figure 2(a). Figure 2(b) shows additional energy dissipation in the hysteresis loops. The overall force-displacement response of the rocking wall system is shown in Figure 2(c). The theoretical background concepts of 'seismic' rocking wall are extensively explained in [9].
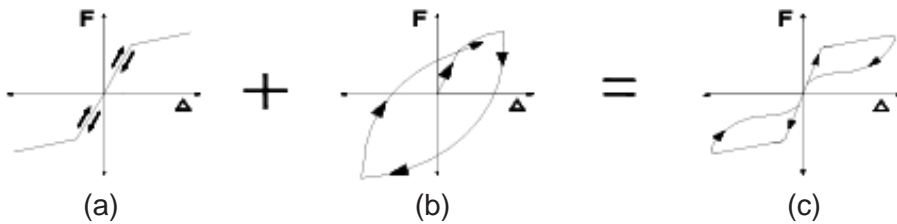

Figure 2   The mechanics of a rocking wall; (a) Bi-Linear Elastic behaviour due to self-weight and unbonded tendons; (b) behaviour of energy dissipators; and (c) hysteresis of flag-shape

Figure 3 presents the detailing of Wall 1 and Wall 2 with different locations of unbonded tendons, fuse-bars and mechanical energy dissipators. Wall 1 was designed with bonded fuse-bars and Wall 2 was designed with unbonded fuse-bars and mechanical energy dissipator. The difference between Wall 1 and Wall 2 is that Wall 1 was constructed with fixed location of tapered fuse-bars and unbonded tendons whilst Wall 2 was built with some performance and configuration flexibilities in terms of location, length, diameter of fuse bars and mechanical energy dissipators.
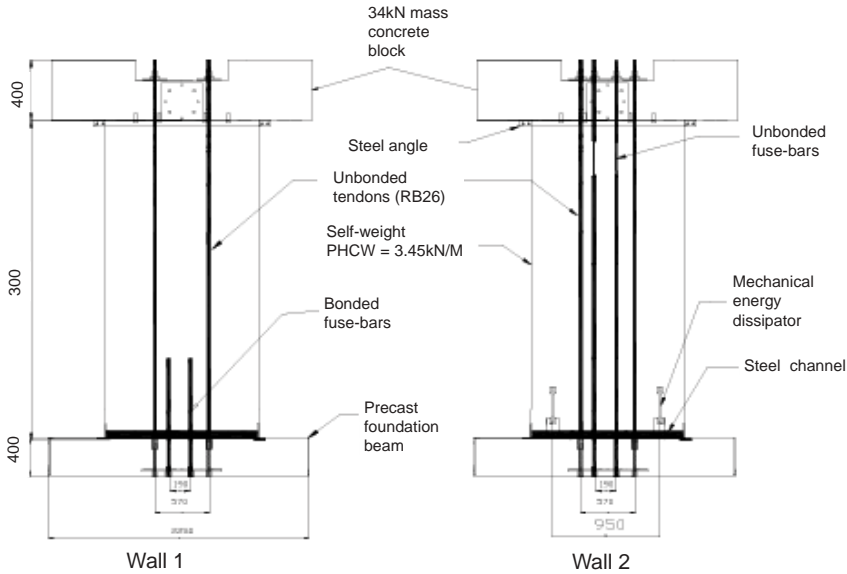
Figure 3   The arrangement of unbonded tendons, fuse-bars and mechanical energy
dissipator in Wall 1 and Wall 2

3.0   EXPERIMENTAL AND THEORETICAL PERFORMANCE OF THE THREE TYPES OF ENERGY DISSIPATORS

Figure 4 shows three different types of energy dissipators used in Wall 1 and Wall 2 together with their experimental results. They are internal fuse-bar, flexural-bending fuse-bar and mechanical energy dissipator. Figure 4(a) shows the stress-strain relationship, the shape, cyclic behaviour and the energy absorption efficiency factor for internal fuse-bar (D1). Fuse bars were machined from reinforcing thread bars (RB25) with measured yield strength of $f_y = 530$ *MPa*. The energy absorption efficiency factor (η) with respect to elasto-perfectly-plastic (EPP) behaviour is defined as:

$$\eta = \frac{E_h}{E_{EPP}} \tag{1}$$

in which E_h= absorbed hysteretic energy observed during a characterisation experiment and E_{EPP}= energy dissipated by a theoretical elasto-perfectly plastic system given by, $E_{EPP} = 2F_y(\Delta_{max} - 2\Delta_y)$. The energy absorption efficiency factor, η for energy dissipator D1 is 0.75, D2 is 0.73 and D3 is 0.71. Figure 4(b) demonstrates the results for the second type of energy dissipator (D2). Flexural beam dissipators were laser-cut from 10 mm thick mild steel plate which had a measured yield strength of $f_y = 300$*MPa*. Figure 4(c) shows the results of externally mounted axial tension mild steel energy dissipator device (D3). The dissipator was laser-cut and machined from a 18 mm thick mild steel plate.
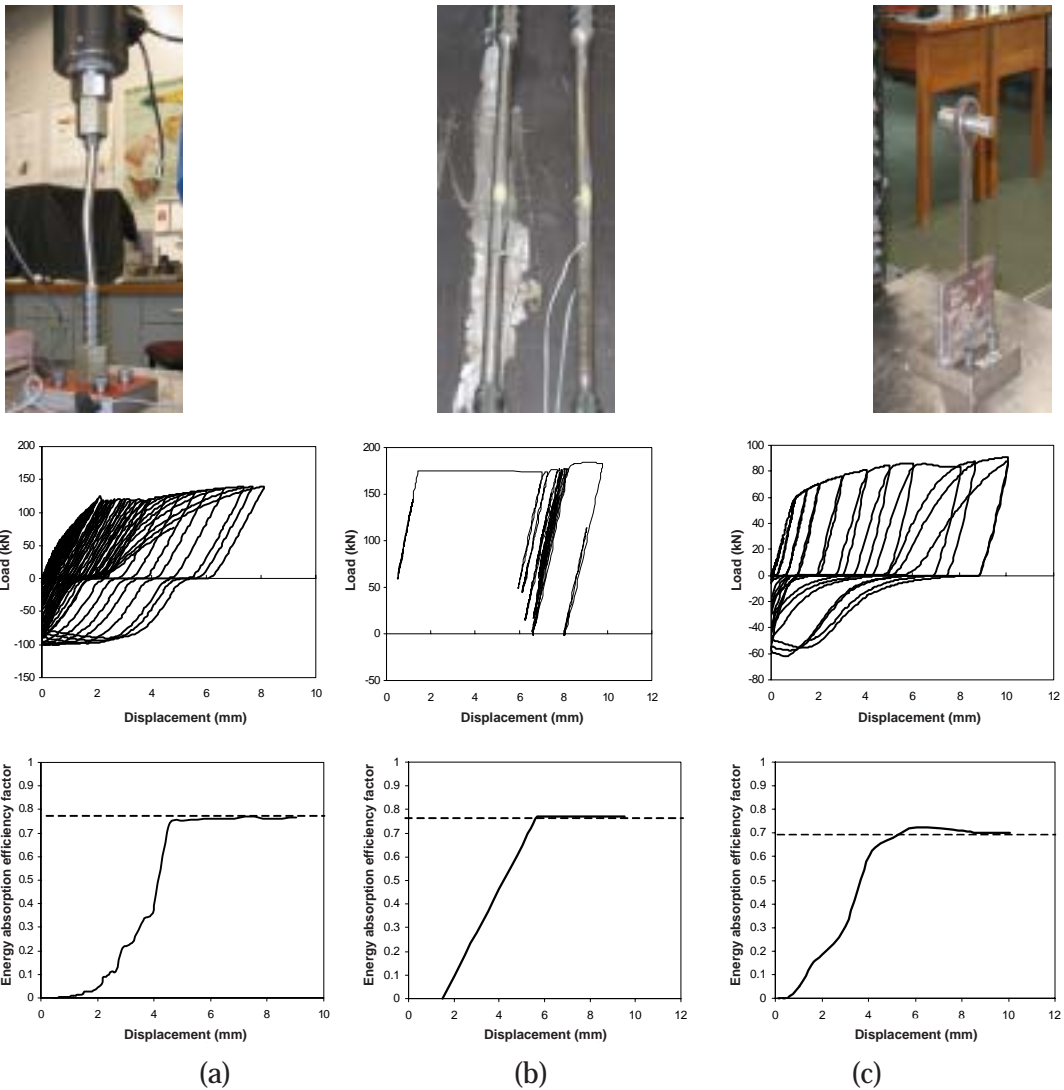
Figure 4 Three different types of energy dissipators showing their stress-strain relationship, shape, cyclic behaviour and energy absorption efficiency factor; (a) internal fuse-bars made from reinforcing thread bar (D1); (b) a pair of mild steel flexural-bending energy dissipators (D2); (c) external mechanical energy dissipator acting as compression-tension yield (D3)

4.0 INSTRUMENTATION, EXPERIMENTAL SET-UP AND TESTING PROCEDURE

Bi-lateral loading experiments were conducted on Wall 1 and Wall 2. The experimental set-up is shown in Figure 5. Figure 5(a) shows the schematic arrangements of wall specimens on shaking table together with reaction frame. A

total number of 27 potentiometers were used to measure in-plane and out-of-plane displacement of wall panels during shaking as shown in Figure 5(b). Six strain gauges were attached to each of the unbonded tendons in order to monitor pretress levels and when yielding occurred. The experimental set-up together with instrumentation is shown in the photograph in Figure 5(c).
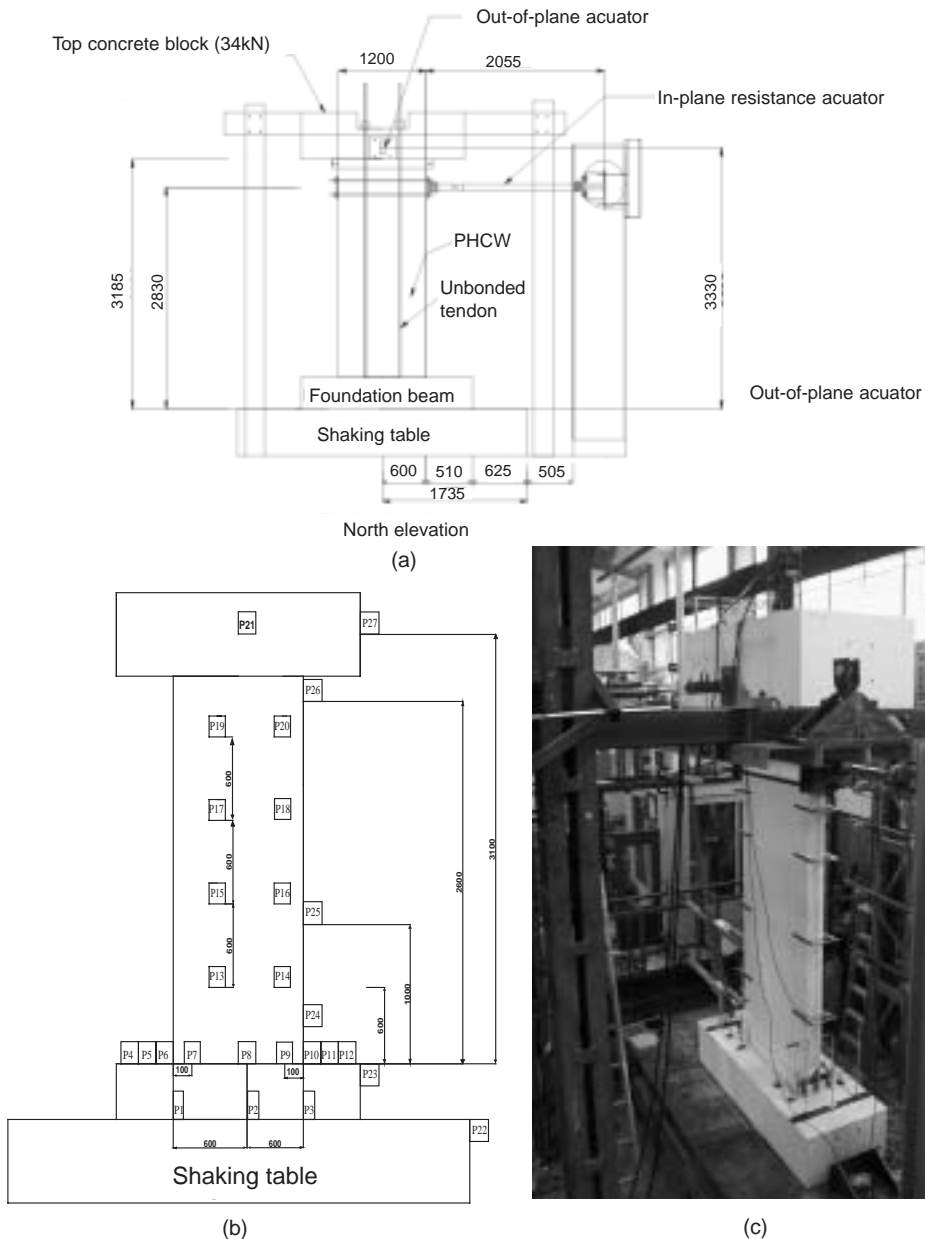

Figure 5 Experimental set-up and instrumentation on shaking table: (a) a schematic loading frame for Wall 1 and Wall 2; (b) instrumentation arrangement for Wall 1 and Wall 2; and (c) the wall specimens ready for testing

5.0 EXPERIMENTAL RESULTS

5.1 Wall 1 Response

Figure 6 represents the overall experimental and theoretical results of seismic bi-lateral performance of Wall 1 at the $\pm 1.5\%$ drift amplitude under the "4-leaf clover" displacement pattern. The location of unbonded tendons, fixed internal fuse-bars (D1), foundation beam and top concrete block of Wall 1 are shown in Figure 6(a). The fixed-based stiffness of the specimen was markedly less than theoretical fixed base (Figure 6(c) and (e)). Figure 6(b) and (d) show the comparison between the predicted and experimental results of bi-lateral load path under "4-leaf clover" displacement pattern. The experimental results followed similar pattern as the predicted results with flat plateau when fixed fuse-bars exceeding yielding strength. Figure 6(f) represents the experimental results for out-of-plane behaviour. Figure 6(h) demonstrated the theoretical out-of-plane behaviour of Wall 1 by taking into account P-Δ effects where ratio of lateral drift (θ_i) over out-of-plane load lies between 0.1 and 0.33. The experimental results showed that there is a linear relationship between out-of-plane load and out-of-plane displacement until at 1.0% drift. But the out-of-plane loading started to decrease as the displacement increase due to the reduction of lateral load affected by gravity loading. Figure 6(i) and 6(g) display the theoretical and experimental "4-leaf clover" displacement controlled pattern, respectively. This pattern was chosen in order to study the extreme seismic behaviour when the out-of-plane loading reached maximum drift while zero drift at in-plane directions or vice-versa. The experimental displacement pattern followed exactly similar to theoretical displacement pattern. It showed that the reaction frames which were in-plane direction (blue frame) and out-of-plane direction (brown frame) stayed stationary during experimental work. Therefore, these experimental results were reliable with minimum percentage of errors.

5.2 Wall 2 Response

5.2.1 Wall 2A

Figure 7 shows the analytical and experimental works under "double 4-leaf clover" pattern at snug-tight, 32% and 64% prestressing of the unbonded tendons without activating any of the energy dissipators. The location of unbonded tendons, foundation beam and top concrete block is shown in Figure 7(a). At snug tight, the test was conducted separately under in-plane direction, out-of-plane and "double 4-leaf clover" pattern as shown in Figure 7(g). Figure 7(i) shows the theoretical values of biaxial "double 4-leaf clover" pattern. Figure 7(e) represents the experimental results of in-plane behaviour of unbonded tendons at $\pm$ 2.0% under 32% level of prestressing. The theoretical in-plane behaviour of wall at 32% prestressing unbonded tendons shows bi-linear relationship after passing the
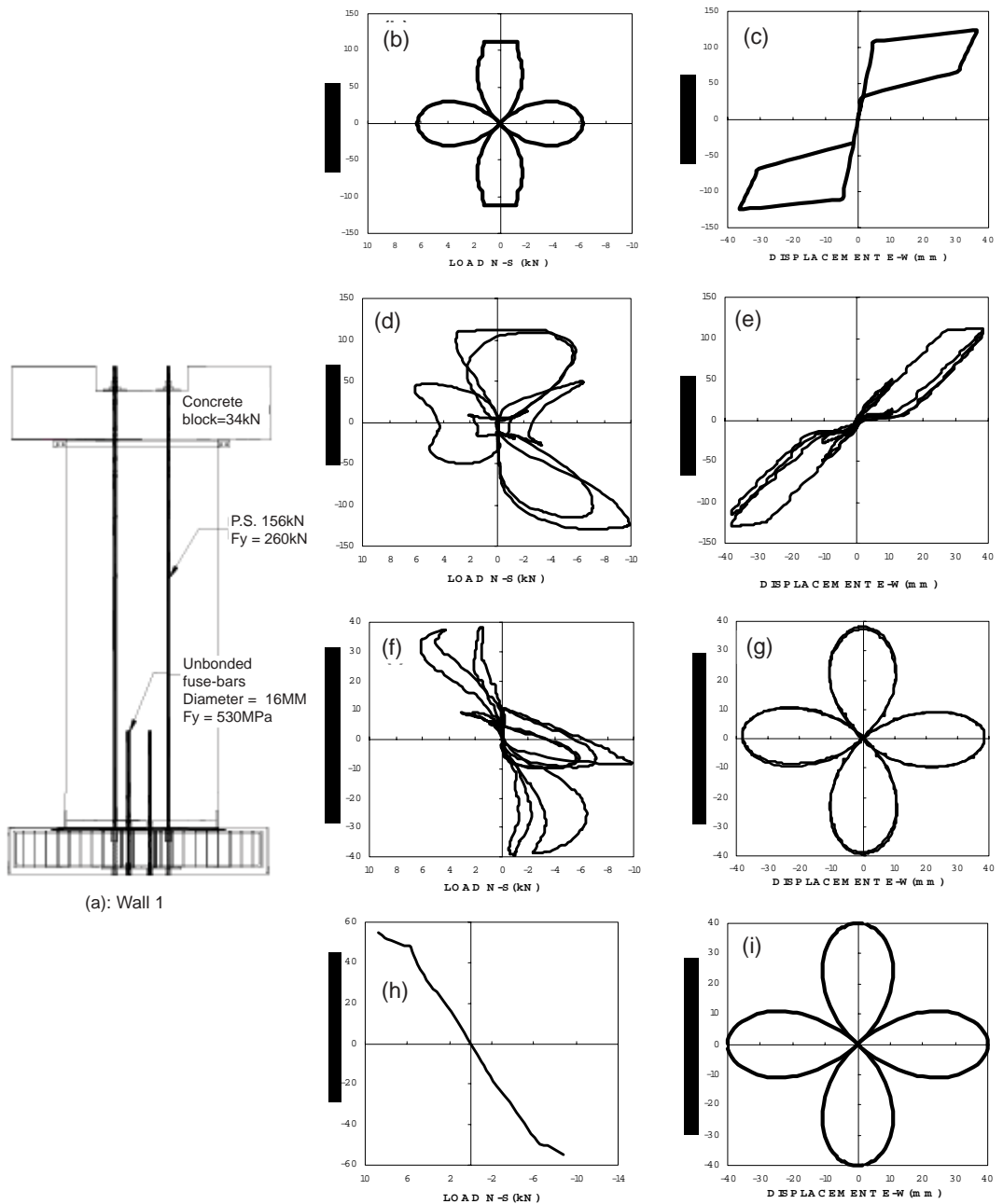
Figure 6   Theoretical and experimental results for Wall 1 at 1.5% drift on shaking table:
(a) combination of Wall 1 with fixed location of energy dissipator and unbonded
tendons; (b) theoretical biaxial load path; (c) theoretical in-plane behaviour;
(d) experimental biaxial loading path; (e) experimental in-plane behaviour; (f)
experimental out-of-plane behaviour; (g) experimental four-clover
displacement pattern; (h) theoretical out-of-plane behaviour; and (i) theoretical
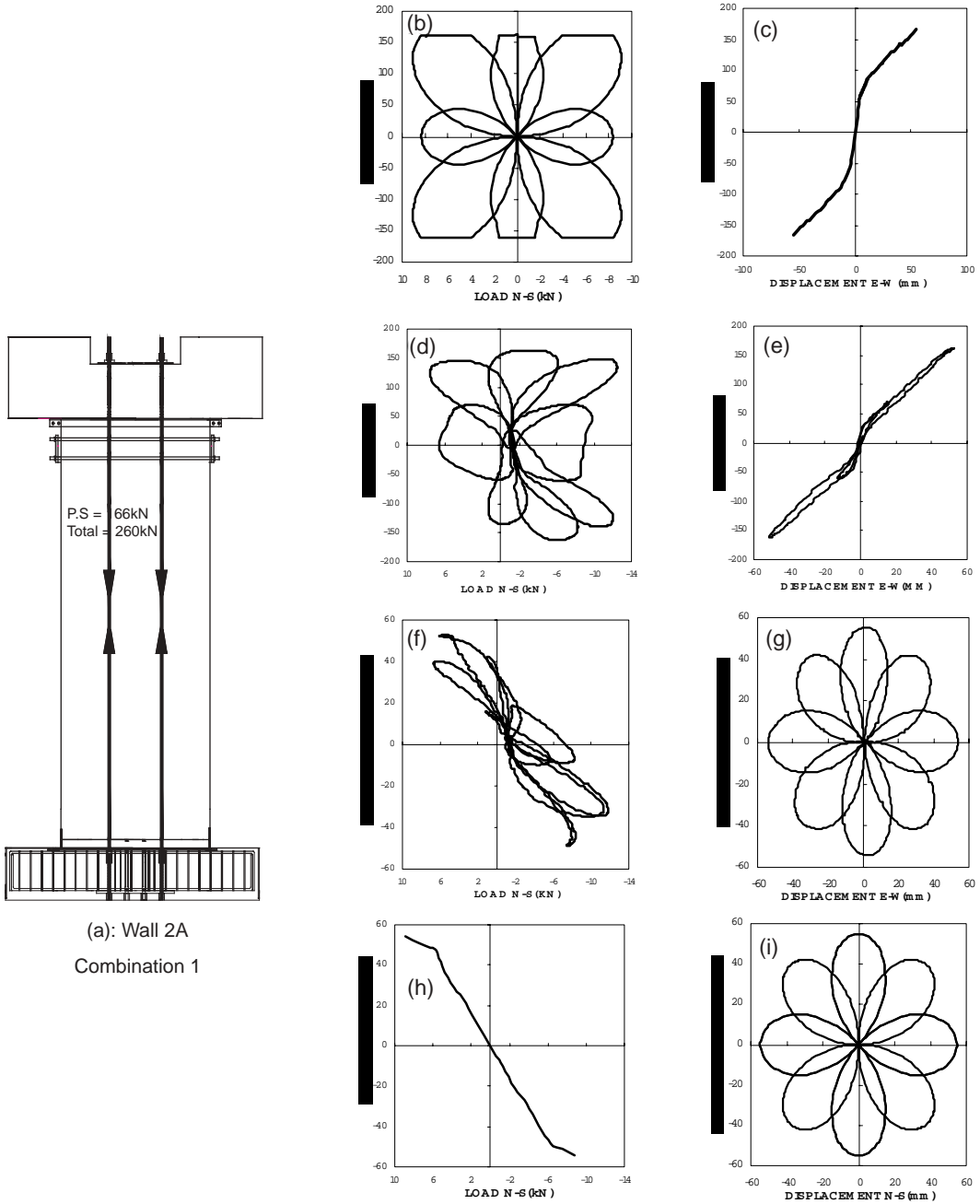four-clover displacement pattern

Figure 7 Theoretical and experimental results of Wall 2A on shaking table: Performance of unbonded tendon only: (a) prestressing 32% and 64% of unbonded tendon; (b) theoretical biaxial loading paths; (c) theoretical in-plane behaviour; (d) experimental biaxial loading path 32% prestressing; (e) experimental in-plane behaviour; (f) experimental out-of plane behaviour; (g) experimental biaxial eight-clover displacement pattern; (h) theoretical out-of-plane behaviour; and (i) theoretical biaxial eight-clover displacement pattern

yielding point as shown in Figure 7(c).The experimental results of "double 4-leaf clover" loading path is shown in Figure 7(d) where both of the unbonded tendons were re-prestressed up to 64%. Wall 2A was tested under in-plane and bi-lateral loadings. The wall started to yield at 0.95% drift and the unbonded tendons lost all their initial prestressing at 2.0% drift. The in-plane lateral load reached strain hardening plateau when both bi-lateral reached maximum displacement and maximum in-plane displacement together with zero out-of-plane displacement. The experimental results have a good agreement with theoretical results as shown in Figure 7(b). The bottom corner of the walls was uplifted by 18.56 mm measured by linear potentiometer at -2.0% drift and western bottom corner was lifted by 16.78 mm (from linear potentiometer) at +2.0%. The creeping sound was heard when the wall went down into the steel base plate because the shear key (pintels) was bent during uplifting out-of-plane loading. The wall was shifted to east about 3.5 mm from its original position due to the sloppiness of shear key. Figure 7(f) and (h) represent the experimental and analytical results for out-of-plane behaviour, respectively. P-Δ effects has greater influence on out-of-plane direction than in-plane direction.

5.2.2 Wall 2B

Figure 8 shows the experimental performance of Wall 2B comprises a pair of unbonded fuse-bars with diameter 16 mm located at the middle of the third and fourth void sections. Initially, fuse-bars were prestressed at 100% followed by 50% from its yielding capacity as shown in Figure 8(a). The characteristic strength of the fuse-bars is similar to that of unbonded tendons because they are made from the same material. Figure 8(e) shows the experimental function of "double 4-leaf clover" displacement controlled pattern. By considering the hysteretic energy dissipated in individual cycles, equivalent viscous damping for Wall 2 can be obtained using the derivation by Chopra [7]. The experimental behaviour of bi-lateral load path for wall using tension fuse-bars only is shown in Figure 8(b). Figure 8(f) represents the equivalent viscous damping, ξ_{eq} of Wall 2B when both fuse-bars were prestressed up to 100%. The calculated values ξ_{eq} for these cycles were coming from in-plane hysteresis loops as shown in Figure 8(c) where first cycle loop is fatter than second cycle. The equivalent viscous damping for in-plane direction only for 50% prestressing of fuse-bars is shown in Figure 8(g). The overall equivalent viscous damping for 50% prestressing is lower than 100% prestressing fuse-bars. For example, equivalent viscous damping for the first cycle of 50% prestressing at 0.5% drift is 2.2% whereas 100% prestressing of fuse bars is 3.1% which means that fuse bars less dissipated energy within the elastic limit. The experimental reduction damping factor, B for 50% and 100% prestressing is shown in Figure 8(h). Figure 8(d) shows the experimental out-of-plane behaviour under "double 4-leaf clover" displacement patterns with some influence of P-Δ effects at
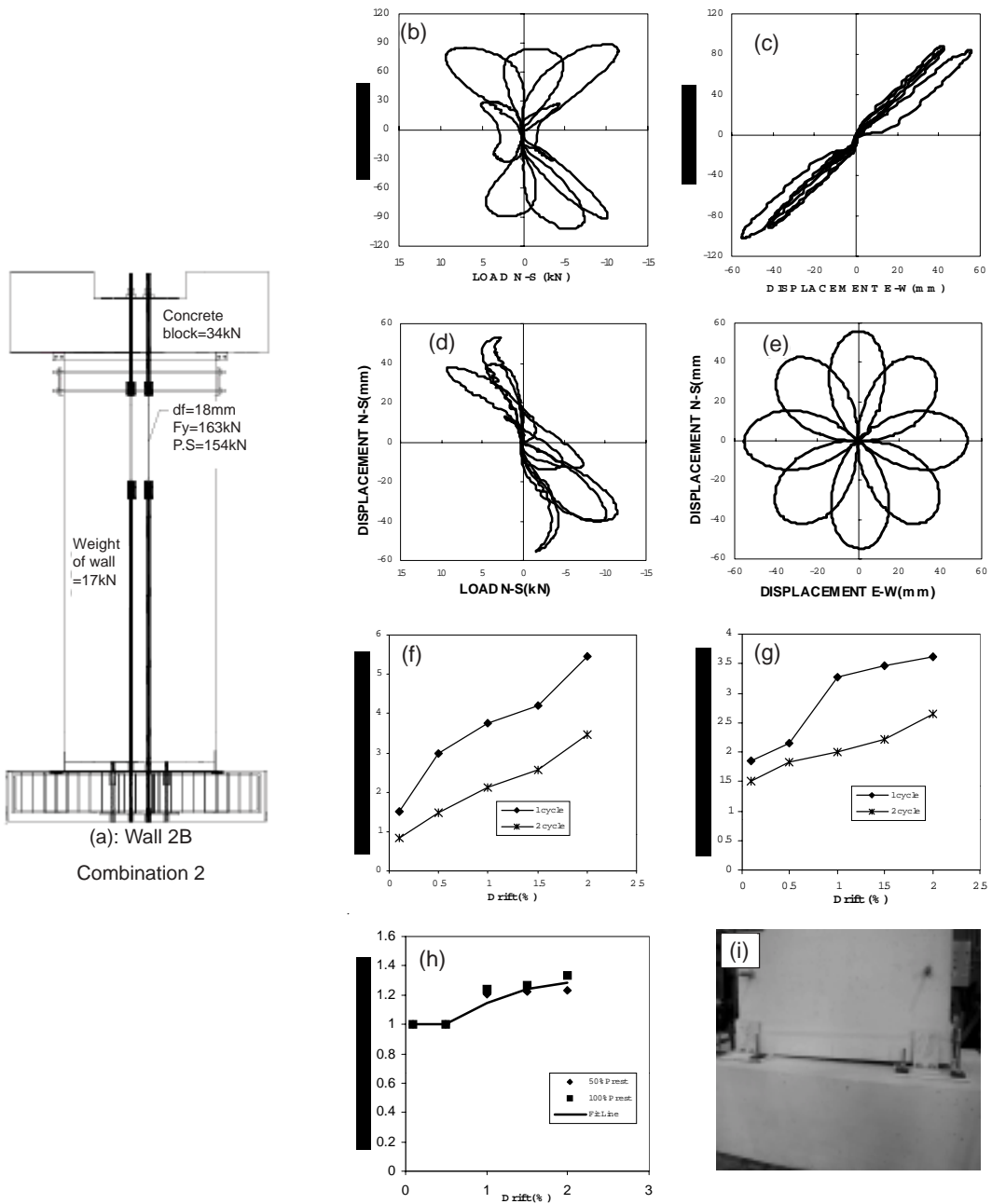
Figure 8 Wall 2 with Combination 2 at ± 2.0% drift: Performance with fuse bars only:
(a) prestressing 100% and 50% of fuse bars; (b) biaxial load path; (c) theoretical
in-plane behaviour; (d) theoretical out-of-plane behaviour; (e) theoretical double
four-leaf clover pattern; (f) equivalent viscous damping for 100% prestressing
fuse bars; (g) equivalent viscous damping for 50% prestressing fuse bars; (h)
the reduction damping factor of the system; and (i) no structural damage at
the bottom of the wall

2.0% drift. Figure 8(i) illustrated that there is no cosmetic and structural damage to the wall. Wall 2B performed very well with significant self-centering forces, no residual displacement and more energy dissipation in the first cycle rather than the second cycle.

5.2.3 Wall 2C

Figure 9 shows the theoretical and experimental performance of Wall 2C under combination of unbonded tendons and unbonded fuse-bars up to 1.5% drift under "double 4-leaf clover" displacement pattern. The arrangement of a pair unbonded tendons and external fuse-bars is shown in Figure 9(a). Wall 2C at Combination 3 with snug tight of unbonded tendons together and 100% or 50% prestressing of fuse-bars were tested subjected to in-plane and bi-lateral quasi-reverse static loading. Initially, both of the fuse bars were prestressed up to 100% and snug-tight unbonded tendons. Figure 9(e) represents the four level of drift at 0.1%, 0.5%, 1.0% and 1.5% under "double 4-leaf clover" displacement pattern. A "flag-shape" behaviour occurred at 1.5% drift where unbonded tendon remained in the elastic region but the fuse bars were in the elasto-plastic region and dissipated most of their energy as shown in Figure 9(c). The bi-lateral loading path is shown in Figure 9(b) followed a similar pattern as eight-clover displacement controlled pattern except at higher drift for E-W direction, the lateral load remain constant. Out-of-plane behave elastically because only a small change in strain in fuse bars and snug tight tendons as shown in Figure 9(d). The wall became more stable with higher base shear because more lateral load required in resisting the forces coming from the combination of unbonded tendons and fuse bars and consequently, less P-Δ effects contributed to out-of-plane behaviour. Figure 9(f) and (g) represent the equivalent viscous damping for in-plane and out-of-plane direction under "double 4-leaf clover" displacement pattern at four cycles. The fourth cycle contributes the highest viscous damping for in-plane directions and third cycle for out-of-plane directions. The overall performance, out-of-plane (N-S direction) has bigger values of viscous damping as compared to in-plane (E-W direction). The scattered values of in-plane and out-of-plane reduction damping factor for four cycles of hysteresis loops and 50% median percentile is shown in Figure 9(h) and (i).

5.2.4 Wall 2D

Figure 10 shows the overall experimental performance of Wall 2D with unbonded tendons and four external mechanical energy dissipators. These mechanical energy dissipators were placed outside of the walls as shown in Figure 10(a). The mechanical energy dissipators were prefabricated, welded to the steel angle and
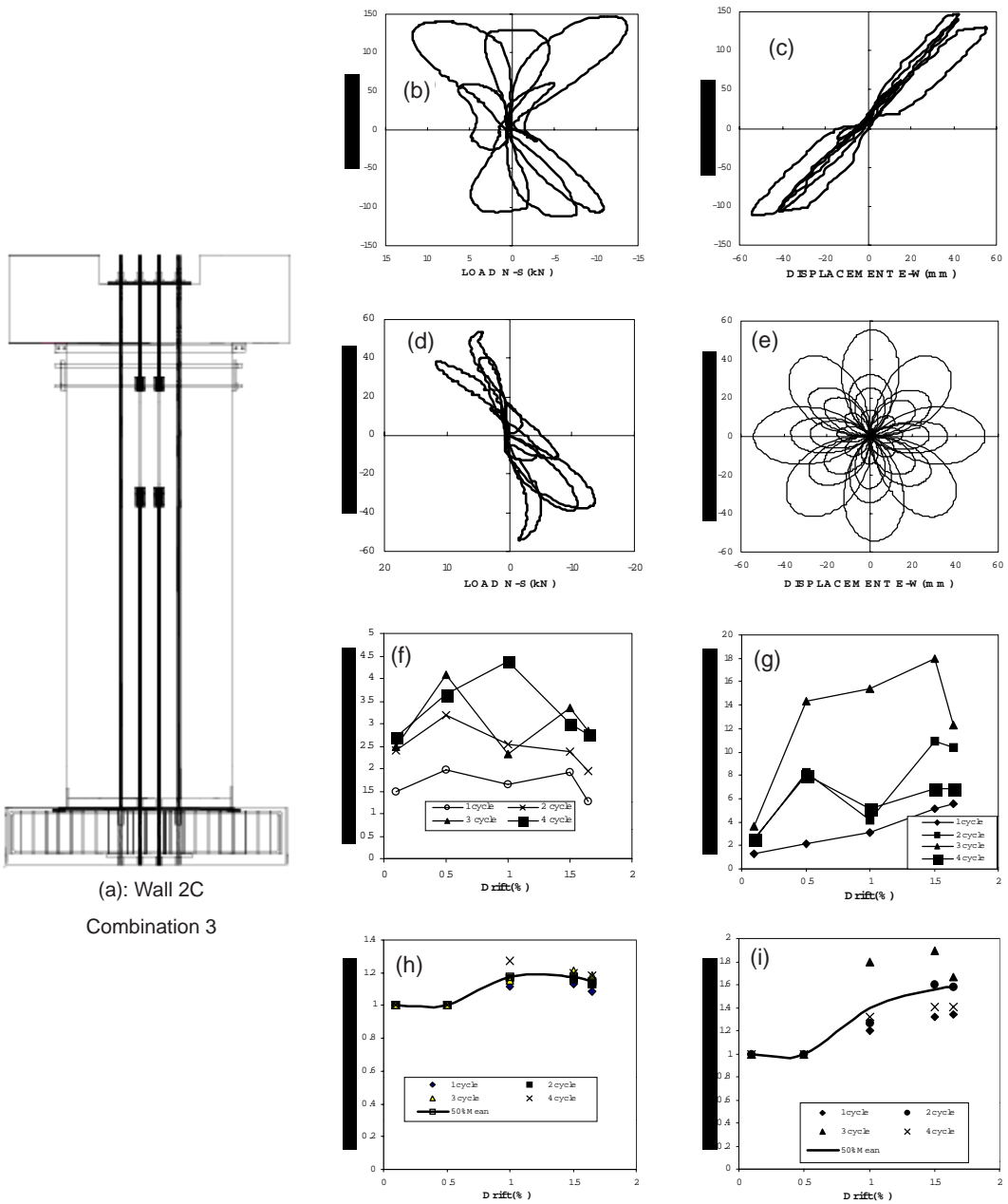
Figure 9 The experimental results of Wall 2C under Combination 3 at ± 2.0% drift: Performance with unbonded tendons and fuse bars: (a) the combination of snug tight unbonded tendons together with 100% and 50% prestressing fuse bars; (b) theoretical bi-lateral loading path; (c) theoretical in-plane behaviour; (d) theoretical out-of plane loading path; (e) theoretical double 4-leaf clover displacement pattern; (f) in-plane equivalent viscous damping; (g) out-of-plane equivalent viscous damping; (h) in-plane reduction damping factor; and (i) out-of-plane reduction damping factor
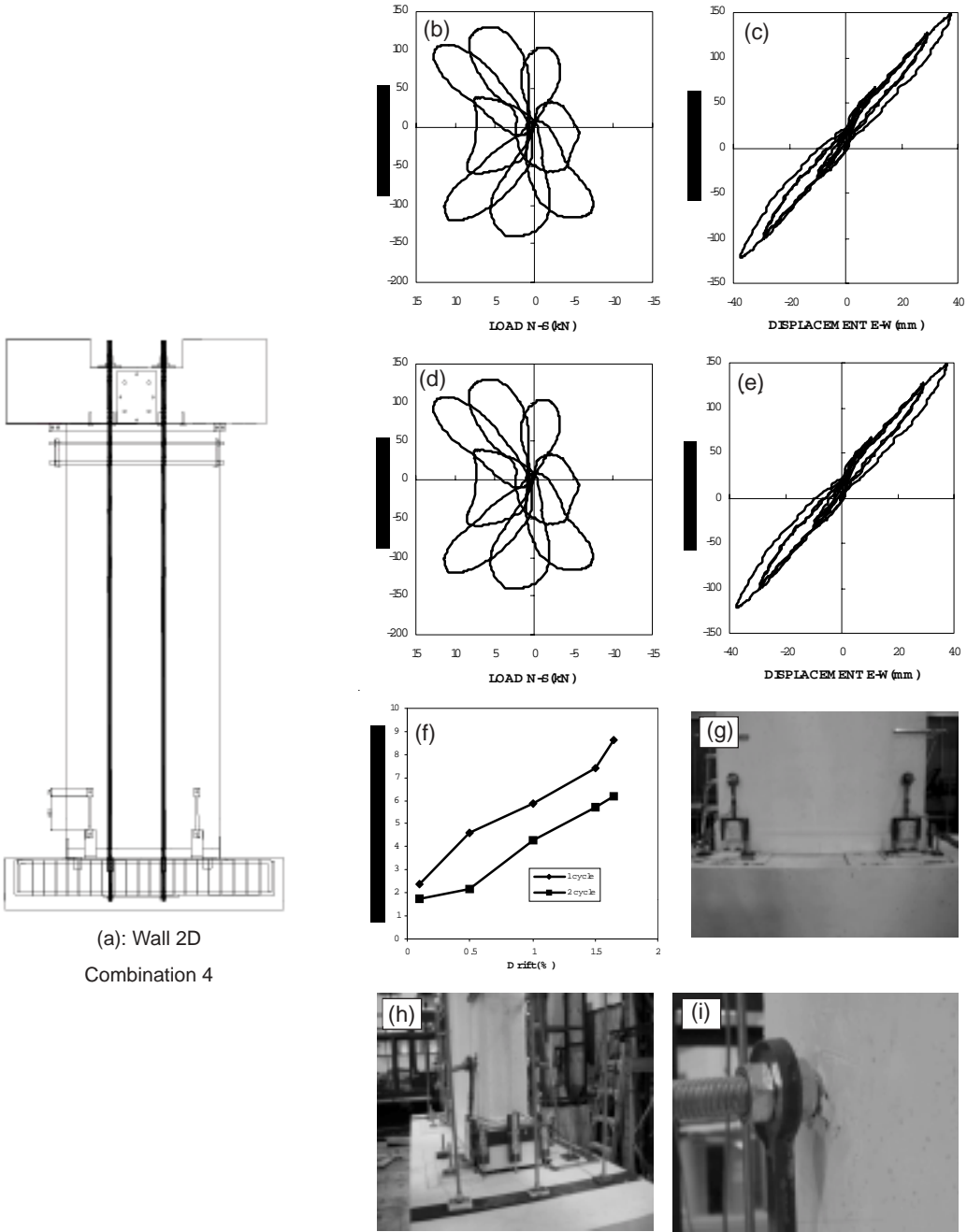
(a): Wall 2D

Combination 4

Figure 10   Wall 2 with Combination 4: Performance with unbonded tendons and mechanical energy dissipators; (a) mechanical energy dissipators with 50% prestressing unbonded tendons; (b) biaxial load path behaviour; (c) in-plane behaviour; (d) out-of-plane behaviour; (e) biaxial eight-clover displacement pattern; (f) in-plane equivalent viscous damping (g) front view of wall; (h) the buckling of energy dissipators; and (i) spalling concrete around the bolts and threaded rods

inserted through the threaded bars as shown in Figure 10(g). Wall 2D was tested using "double 4-leaf clover" pattern as depicted in Figure 10(e) up to 1.5% drift. When the drift increases up to 1.5%, the concrete around the threaded bars started to peel off and crack line was observed around the bolt as demonstrated in Figure 10(i). At the end of the test, all the mechanical energy dissipators were buckled and bent toward the wall as illustrated in Figure 10(h). This phenomenon occurred due to un-prestressed state of mechanical energy dissipators and activated under tension-compression element where the buckling problem occurred when exceeding the yielding strength and related to their slenderness ratio of Euler equation. The mechanical energy dissipator dissipates most of their energy as compared to Wall 2B and Wall 2C. The cross-sectional area of one mechanical energy dissipator is 256 mm^2 with yield strength, $f_y = 300$ MPa. This cross-section was chosen based on moment contribution of mild steel which could produce the same amount of moment from high yield fuse-bars. The "banana-shape" of in-plane behaviour of Wall 2D is shown in Figure 10(c) where the mechanical energy dissipator yielded in tension and buckled in compression. The overall bi-lateral performance behaviour under this type of loading is shown in Figure 10(b). The experimental performance of out-of-plane behaviour is shown in Figure 10(d). Figure 10(f) shows the equivalent viscous damping for in-plane direction for two cycles of loading. Even though this type of energy dissipators released most of their energy as compared to other types of energy dissipators, but it is not recommended in rocking precast hollow core wall system due to buckling and aesthetic problems.

6.0 CONCLUSIONS & RECOMMENDATIONS

Based on the experimental study on a single rocking precast prestressed concrete hollow core wall unit presented herein the following conclusions are drawn:

(i)   The experiments have demonstrated that precast prestress concrete hollow core units can be used as a viable alternative to solid reinforced concrete walls. This is so in spite of the lack of any transverse reinforcement for shear resistance. This gives a wider scope for the use of hollow core units which have customarily been used mostly for floor units in buildings.

(ii) The success of the rocking hollow core walls that requires carefully detailed armouring at the base of the wall to enable high point load stresses to be dispersed up the wall and also into the foundation.

(iii) Rocking walls in themselves dissipate little energy, but this can be improved through the used of supplemental energy dissipators. The dissipators tested in this study each had advantages and disadvantages. It would appear that the best approach is to use prestressed fuse-bars only as these always keep

the wall clamped firmly to the foundation when not rocking. Other dissipator types can cause the walls to "sit up" on the devices when they yield, this effectively softens the structure.

(iv) By providing pintels or shear keys at bottom corner of walls, the seismic lateral base shear can be resisted by rocking without sliding. No transverse reinforcement in precast hollow core walls need be used. In the present study, to help improve shear resistance at the base of the wall, the hollow core voids were filled to a height equivalent to one unit width (1.2 m). Future research could potentially show that this extent of infilling would be relaxed.

REFERENCES

[1]   Fintel, M. 1995. Performance of Buildings with Shear Walls in Earthquake in the Last Thirty Years. *PCI Journal.* 40(3): 62-80.

[2]   Wood, S., J. Wright, and J. Moehle. 1987. The 1985 Chile Earthquake, Observations on Earthquake-Resistant Construction in Vina del Mar. Civil Engineering Studies, Structural Research Series No. 532. University of IIlinois, USA.

[3]   Wyllie Jr, L. A. and J. R. Filson. 1989. Armenia Earthquake Reconnaissance Report. Earthquake Spectra. Special Supplement (August 1989).

[4]   Berg, G. V. and J. L. Stratta. 1964. Anchorage and the Alaska Earthquake on March 27, 1964. American Iron and Steel Institute. 63.

[5]   Holden, T. J., J. Restrepo, and J. B. Mander. 2003. Seismic Performance of Precast Reinforced and Prestressed Concrete Walls. *Journal of Structural Engineering, ASCE.* 4(5): 286-296.

[6]   Mander, J. B. and C.-T. Cheng. 1997. Seismic Resistance of Piers Based on Damage Avoidance Design. Technical Report NCEER-97-0014. State University of New York at Buffalo, Department of Civil, Structural and Environmental Engineering. Buffalo, New York, U.S.A.

[7]   Copra, A. L. 2001. *Dynamic of Structures: Theory and Applications to Earthquake Engineering.* Second Edition, Upper Saddle River: Prentice Hall.

[8]   Lin,Y. Y. and K. C. Chang. 2004. Effects of Site Classes on Damping Reduction Factors. *Journal of Structural Engineering, ASCE.* 133(9): 1667-1675.

[9]   Hamid, N. H. 2006. Seismic Damage Avoidance Design of Warehouse Buildings Constructed using Precast Hollow Core Panels. Ph.D. Thesis. Department of Civil Engineering, University of Canterbury. Christchurch, New Zealand.